Nonlinear Dynamics and Systems Theory, **20** (2) (2020) 144–152

# Chaos in New 2-d Discrete Mapping and Its Application in Optimization

R. Bououden [1*], M. S. Abdelouahab [1] and F. Jarad [2]

[1] *Laboratory of Mathematics and their Interactions, Abdelhafid Boussouf University Center, Mila, Algeria.*
[2] *Department of Mathematics, Faculty of Arts and Sciences, Cankaya University, Ankara, Turkey.*

Received: November 24, 2019; Revised: March 5, 2020

**Abstract:** In this paper, we propose a new map which is a combination of the Hénon and Lozi maps. We analyze the proposed map numerically and with the aid of bifurcation plots. On the other hand, and as an example of application of this new map, we are going to use it in the chaotic optimisation algorithm. To prove the efficiency of this map, we use numerical results thorought the paper.

**Keywords:** *chaos optimization; test functions; Hénon map; Lozi map.*

**Mathematics Subject Classification (2010):** 34H05, 34K35.

## 1 Introduction

Recently, a large number of complex nonlinear optimization problems are solved using chaotic optimization algorithms [2–6]. In such cases, traditional algorithms [7–10] may not often produce the desired outcomes and therefore alternate methods must be employed.

For the last few decades, researchers have focused on developing hybrid algorithms by combining heuristic algorithms with chaos searching techniques to solve a non-linear system of equations and optimization problems such as the chaotic Monte Carlo optimization, chaotic BFGS, chaotic particle swarm optimization, chaotic genetic algorithms, chaotic harmony search algorithm, chaotic simulated annealing, gradient-based methods and so on [11–13]. Due to the non-repetition of chaos, the chaotic optimization algorithm can carry out overall searches at higher speeds than the stochastic ergodic searches that depend on probabilities.

* Corresponding author: mailto:rabouden@yahoo.fr

© 2020 InforMath Publishing Group/1562-8353 (print)/1813-7385 (online)/http://e-ndst.kiev.ua

Different types of chaotic systems have been considered in literature for applications in optimization methods. The logistic equation and other equations, such as the tent map, Gauss map, Lozi map, Hénon map, sinusoidal iterator, Chua's oscillator, Ikeda map, and others, have been adopted instead of the random ones with very interesting results [14–17].

The most popular map which is used in chaotic optimization algorithm is the Hénon map [18]. M. Hénon has defined a map from the plane to itself. It is one of the most studied examples of dynamical systems that exhibit chaotic behaviour. The Hénon map is defined by

$$H\begin{pmatrix} x \\ y \end{pmatrix} = \begin{pmatrix} 1 - ax^2 + by \\ x \end{pmatrix}. \tag{1}$$

For $a = 1.4$ and $b = 0.3$, the Hénon map (1) is chaotic as in Figure 1 (a). For other values of $a$ and $b$, the map may be chaotic or converge to a periodic orbit.

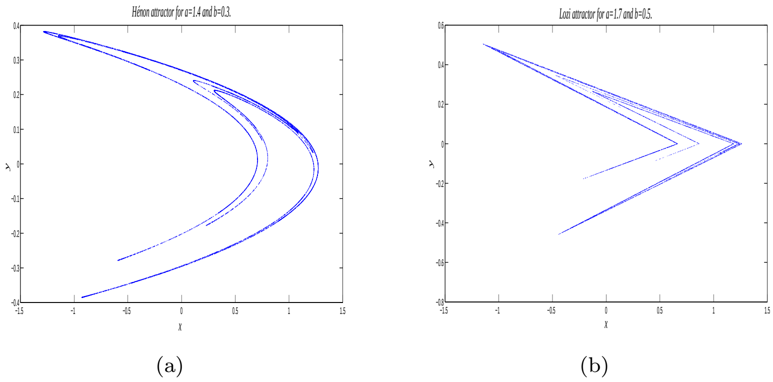


**Figure 1**: (a) The Hénon attractor obtained for $a = 1.4$ and $b = 0.3$. (b) The Lozi attractor obtained for $a = 1.7$ and $b = 0.5$.

In 1978, Lozi introduced a two-dimensional map (2), see [19], where he replaced the quadratic term in the Hénon map (1) by a piecewise linear one

$$L\begin{pmatrix} x \\ y \end{pmatrix} = \begin{pmatrix} 1 - a \mid x \mid + by \\ x \end{pmatrix}. \tag{2}$$

This map displays a chaotic attractor for $a = 1.7$ and $b = 0.5$ as in Figure 1 (b).

In this paper we propose a new map which is a combination of the Hénon and Lozi maps and we use it to find solutions of complex optimization problems.

## 2 The New Proposed Map

Because we need a map that has a very complex behaviour to be used in the optimization algorithm as mentioned in the previous section, we suggest the following new map:

$$HL\begin{pmatrix} x \\ y \end{pmatrix} = \begin{pmatrix} 1 - ax^2 + by \\ 1 - a \mid y \mid + bx \end{pmatrix}, \tag{3}$$

where $a$, $b$ are the bifurcation parameters.

## 3 Bifurcation and Chaos

In this section, the dynamical behaviour of system (3) will be investigated numerically. We recall that the Lyapunov exponents of an attractive periodic orbit are negative. Also, a periodic point can only bifurcate if at least one of its Lyapunov exponents is zero. Finally, if at least one of the Lyapunov exponents is positive, then the behaviour of the map becomes chaotic.

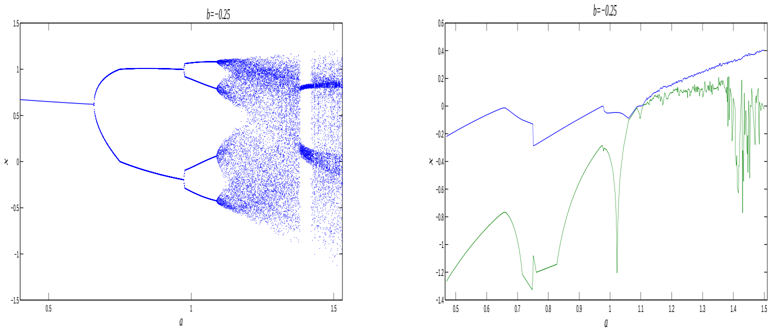


(a) (b)

**Figure 2**: (a) Bifurcation diagram for $b = -0.25$ and $0.4 < a \leqslant 1.5$. (b) Variation of the Lyapunov exponents versus the parameter $0.4 < a \leq 1.5$, with $b = -.025$.

For $b = -0.25$ and $0.4 < a < 1.53$ we can see different bifurcations of map (3) as shown in Figure 2 (a). In the interval $0.4 < a < 0.658$, map (3) converges to a stable fixed point. The first bifurcation occurs at $a = 0.659$ from the fixed point to a period-2 orbit. This period-2 orbit arises out of a period-doubling bifurcation [2]. Then, along the interval $0.659 \leq a < 0.974$, map (3) converges to a stable period-2 orbit. When $a = 0.975$, the second bifurcation (period-doubling bifurcation) occurs from the period-2 orbit to a stable period-4 orbit. The third bifurcation happens when $a = 1.08925$ from period-4 orbit to a full chaotic behaviour. These bifurcations seem very clear in Figure 2 (b), where we notice that the Lyapunov exponents are both negative on the interval $0.4 < a < 1.0892$ except at the bifurcation points $a = 0.659$, $a = 0.975$ and $a = 1.08925$, where one of the Lyapunov exponents is zero. This means that map (3) converges to the periodic orbit on the interval $0.4 < a < 1.0892$. In the interval $1.0893 < a < 1.53$ it converges to a chaotic attractor and this is clear in Figure 2 (b), where one of the Lyapunov exponents is positive. Figure 4 (a) shows an example of the chaotic attractor that appears when $1.0893 < a < 1.53$.

Similarly, as we see in Figure 3 (a), for the fixed $a = 0.95$ and $-0.9487 \leq b \leq 0.4474$, the behaviour of map (3) takes different shapes. On the interval $-0.9487 \leq b < -0.8135$, map (3) converges to the chaotic attractor (one of the Lyapunov exponents is positive as in Figure 3 (b). As an example of the chaotic attractor that appears when $-0.9487 \leq b < -0.8135$, we have Figure 4 (b). In the interval $-0.9488 < b \leqslant 0.177$ we have a series of bifurcations of the types of the period-doubling bifurcation as in Figure 3 (a) and (b). Get back again to a chaotic behaviour when $0.1773 < b \leq 0.2117$. When $b = 0.2118$, we have a new bifurcation from the chaos behaviour to a period-14 orbit. When $b$ exceeds the value $b = 0.253$, map (3) converges to a chaotic attractor (Figure 4 (b)).

The advantage of the proposed map is that it possesses rich dynamical properties such

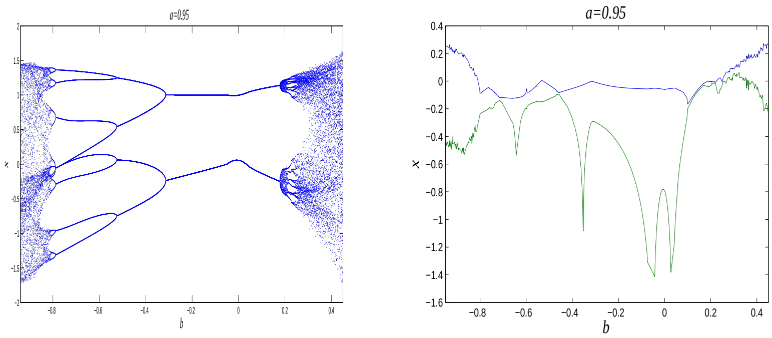


(a) (b)

**Figure 3**: (a) Bifurcation diagram for $a = 0.95$ and $-0.94 < b \leqslant 0.45$. (b) Variation of the Lyapunov exponents versus the parameter $-0.94 < b \leq 0.45$, with $a = 0.95$.

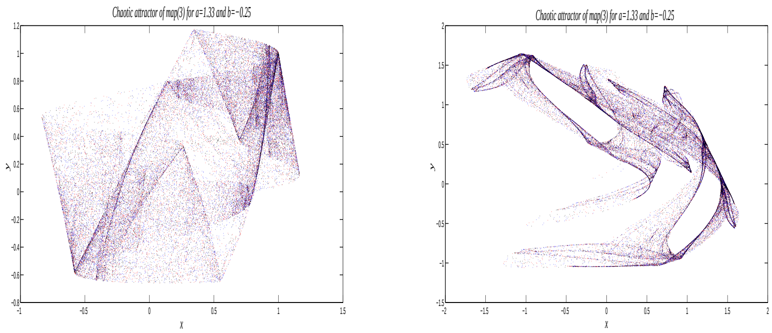


(a) (b)

**Figure 4**: (a) Chaotic attractor of map (3) obtained for $a = 1.33$ and $b = -0.25$. (b) Chaotic attractor of map (3) obtained for $a = 0.95$ and $b = 0.44$.

as fixed points of different types, periodic orbits of different periods and strange attractors which are completely different from all the attractors observed in the behaviour of maps (1) and (2).

## 4 Pure Chaotic Optimization Algorithm Based on Map (3)

In [2], Bououden R. and Abdelouahab M.S. have used a sampling mechanism to coordinate the research methods based on chaos theory by using the Lozi map. The obtained results show that the $PCOA$ algorithm is fast and converges to a good optimum. In this paper we use map (3) to solve some optimization problems.

In the following we are going to describe the pure chaotic optimization algorithm.

**Algorithm 4.1**

**Inputs:**

$N$**:** max number of iterations of chaotic global search.

$N_p$**:** max number of packets of global search.

$M_g$**:** max number of iterations of chaotic global search for any packets.
$M_{gl}$**:** max number of iterations of chaotic local search in global search.
$M_l$**:** max number of iterations of chaotic local search.
$Mt = N_p(M_g M_{gl} + M_l)$**:** stopping criterion of chaotic optimization method in iterations.
$\lambda_{gl}$**:** the width of the interval in chaotic local search in global search.
$\lambda$**:** the width of the interval in chaotic local search.
**Outputs:**
$\bar{x}$**:** best solution from current run of chaotic search.
$\bar{f}$**:** best objective function (minimization problem).
**Step 1:** Initialization of the numbers $M_g$, $M_{gl}$, $M_l$ of the steps of chaotic search and initialization of the parameters $\lambda_{gl}$, $\lambda$ and initial conditions. The Lozi map (2) is adopted to have a chaotic behaviour in order to use it for generating several sequences of points by using different initial conditions (the number of sequences is equal to the dimension of the objective function) after every sequence $\{y(i), i = 1, 2, ...n\}$ is normalized in the range $[0, 1]$ as follows:

$$z(i) = \frac{y(i) - \alpha}{\beta - \alpha} \tag{4}$$

for all $i = 1, 2, ...n$, where $\alpha = min\{(y(i), i \geq 1\}$, $\beta = max\{(y(i), i \geq 1\}$.
**-Step 2-1: Algorithm of chaotic global search:**
**for** $t = 1 : N_p$
Set the initial best objective function $\bar{f(t)} = +\infty$.
**while** $k \leq M_g$ **do**
$x_i(k) = L_i + z_i(k)(U_i - L_i)$, $i = 1, 2, ..., n$
**if** $f(x(k)) < \bar{f}$, **then**
$\bar{x} = x(k)$, $\bar{f} = f(x(k))$
**- Step 2-2: Sub algorithm of chaotic global-local search:**
Transform the points generated by Lozi map in the neighbourhood of the point $\bar{x}$ and we begin the search
**while** $j \leq M_{gl}$ **do**
**if** $f(x(j)) < \bar{f}$, **then**
$\bar{x} = x(j)$, $\bar{f} = f(x(j))$
**end if**
$j = j + 1$
**end while**
**end if**
$k = k + 1$
**end while**
**end for**
**- Step 3: Algorithm of chaotic local search:**
Transform the points generated by logistic map in the neighbourhood of the point $\bar{x}$ and we begin the search
**while** $k \leq M_l$ **do**
**if** $f(x(k)) < \bar{f}$, **then**
$\bar{x} = x(k)$, $\bar{f} = f(x(k))$
**end if**
$k = k + 1$
**end while**

During the chaotic local search, the step size $\lambda$ (resp $\lambda_{gl}$) is an important parameter in convergence behaviour of the optimization method which adjusts small ergodic ranges around $X_*$. The step sizes $\lambda$ and $\lambda_{gl}$ are employed to control the impact of the current best solution on generating a new trial solution. The small $\lambda$ and $\lambda_{gl}$ tend to perform exploitation to refine results by local search, while the large ones tend to facilitate a global exploration of search space.

## 5 Experimental Results and Analysis

### 5.1 Some test functions

To validate the effectiveness of this new map in solving optimization problems we use it with the PCOA proposed in [2] in order to search for optimal solutions of the following benchmark functions.

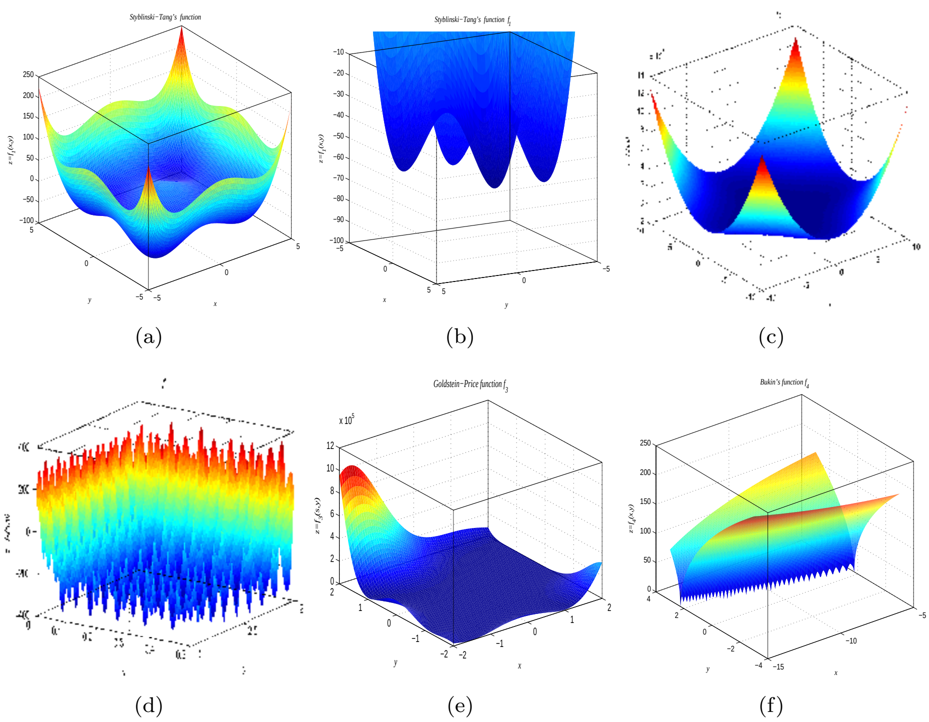


**Figure 5**: (a) The Styblinski-Tang function $f_1$. (b) Magnification of the Styblinski-Tang function $f_1$. (c) Function $f_2$. (d) Magnification of function $f_2$. (e) The Goldstein-Price function $f_3$. (f) The Bukin function $f_4$.

1.

$$f_1(x_1, x_2, ..., x_n) = \frac{\sum_{i=1}^{n}(x_i^4 - 16x_i^2 + 5x_i)}{2},$$

where $-5 \le x_i \le 5$ for $1 \le i \le n$.

2.

$$f_2(x_1,x_2) = x_1^4 - 7x_1^2 + x_2^4 - 9x_2^2 - 5x_2 + 11x_1^2x_2^2 + 99\sin(71x_1) + 137\sin(97x_1x_2) + 131\sin(51x_2),$$

where $-10 \leq x_1 \leq 10$ and $-10 \leq x_2 \leq 10$.

3.

$$f_3(x_1,x_2) = [1 + (x_1 + x_2 + 1)^2(19 - 14x_1 + 3x_1^2 - 14x_2 + 6x_1x_2 + 3x_2^2)]\times [30 + (2x_1 - 3x_2)^2(18 - 32x_1 + 12x_1^2 + 48x_2 - 36x_1x_2 + 27x_2^2)],$$

where $-2 \leq x_1 \leq 2$ and $-2 \leq x_2 \leq 2$.

4.

$$f_4(x_1,x_2) = 100\sqrt{|x_2 - 0.01x_1^2|} + 0.01\,|x_1 + 10|\,,$$

where $-15 \leq x_1 \leq -5$ and $-3 \leq x_2 \leq 3$.

Figures 5 (a) and (b) show the 3D plots of the Styblinski-Tang function $f_1$ which is a $d$-dimensional function, usually evaluated on the hypercube $x_i \in [-5,5]$, for all $i = 1, ..., d$. It has a global minimum

$$-39.16617 \times d \leq f_4(-2.903534, ..., -2.903534) \leq -39.16616 \times d.$$

Concerning $f_2$ shown in Figures 5 (c) and (d), it possesses hundreds of local minima [2], but its global minimum is not yet theoretically known.
$f_3$ is the Goldstein-Price function usually evaluated on the rectangle

$$(x_1,x_2) \in [-2,2] \times [-2,2],$$

it has a lot of local minima and one global minimum $f_3(0,-1) = 3$ and the 3D plot of this function is in Figure 5 (e).
$f_4$ is the Bukin function which is usually evaluated on the rectangle

$$(x_1,x_2) \in [-15,-5] \times [-3,3],$$

it has a lot of local minima and one global minimum $f_4(-10,1) = 0$, see Figure 5 (f).

### 5.2 Numerical experiments

In order to enrich our study, we are going to use different values of the step sizes $\lambda$, $\lambda_{gl}$, different values of the number of iterations $M_g$, $Mgl$ and $M_l$ as in Table 1 and different values of the max number of packets of global search $N_p$ presented in Table 1. Each optimization code was implemented in Matlab (MathWorks). All the codes were run on a 2.53 GHz, i3 processor with 4 GB of random access memory.

Table 2 shows the numerical results of the global minima research of the test functions $f_1$, $f_2$, $f_3$ and $f_4$.

For the Styblinski-Tang function $f_1$, the best result is $-117.4985$ and we got it by using the Lozi map and Lozi-Hénon map. Concerning the function $f_2$, the best result is $-395.8756$ and we got it by using the Lozi-Hénon map. The Lozi-Hénon map gave the best results for the optimization problem of $f_3$ in common with the Lozi map. Again, the Lozi-Hénon map gave the best results (0.0049) of the optimization problem of $f_4$.

| | $\lambda$ | $\lambda_{gl}$ | $N_p$ | $M_g$ | $M_{gl}$ | $M_l$ |
|---|---|---|---|---|---|---|
| C1 | 0.001 | 0.01 | 100 | 10 | 100 | 100 |
| C2 | 0.002 | 0.05 | 100 | 100 | 200 | 200 |
| C3 | 0.005 | 0.08 | 1000 | 100 | 200 | 200 |

**Table 1**: The set of parameter values for every run of the PCOA algorithm.

| Function | Cases | $LPCOA$ | $HPCOA$ | $LHPCOA$ | Best map |
|---|---|---|---|---|---|
| $f_1$ | $C1$ | −117.4772 | −116.2624 | −117.3158 | Lozi and Lozi-Hénon |
| | $C2$ | −117.4924 | −117.1878 | −117.4979 | |
| | $C3$ | −117.4985 | −117.4981 | −117.4985 | |
| $f_2$ | $C1$ | −390.2672 | −394.5880 | −385.7419 | Lozi-Hénon |
| | $C2$ | −395.8622 | −395.6099 | −395.8374 | |
| | $C3$ | −395.8742 | −395.8641 | −395.8756 | |
| $f_3$ | $C1$ | 3.0000 | 3.1689 | 3.0000 | Lozi and Lozi-Hénon |
| | $C2$ | 3.0000 | 3.0000 | 3.0000 | |
| | $C3$ | 3.0000 | 3.0000 | 3.0000 | |
| $f_4$ | $C1$ | 0.0322 | 0.0371 | 0.0310 | Lozi-Hénon |
| | $C2$ | 0.0108 | 0.0096 | 0.0071 | |
| | $C3$ | 0.0086 | 0.0145 | 0.0049 | |

**Table 2**: Optimization results over one run for 3 parameter configurations using the PCA algorithm with three different maps (The Lozi map, Hénon map and Lozi-Hénon map).

## 6 Conclusion

This paper reported the results of a study of a new 2-d map derived from the Lozi and Hénon maps by mixing between them. The fixed points, periodic orbits and chaotic behaviour of the new 2-d map are analysed by means of the bifurcation diagrams. On the other hand, this paper gives an application of this new map to the optimization problems with a comparison study to the Lozi and Hénon map findings. The results obtained show that the Lozi-Hénon map yields better results than the Lozi and Hénon maps.

## Acknowledgment

This research was supported by the Algerian General Directorate for Scientific Research and Technological Development (DGRSDT).

## References

[1] M. F. Hassan and E. K. Boukas. Constrained linear quadratic regulator: continuous-time case. *Nonlinear Dynamics and Systems Theory* **8** (1) (2008) 35–42.

[2] R. Bououden and M. S. Abdelouahab. On Efficient Chaotic Optimization Algorithm Based on Partition of Data Set in Global Research Step. *Nonlinear Dynamics and Systems Theory* **18** (1) (2018) 42–52.

[3] S. F. Woon., V. Rehbock and R. C. Loxton. Global Optimization Method for Continuous-Time Sensor Scheduling. *Nonlinear Dynamics and Systems Theory* **10** (2) (2010) 175–188.

[4] M. Marko., V. Najdan., P. Milica and M. Zoran. Chaotic fruit fly optimization algorithm. *Knowledge-Based Systems* **89** (2015) 446–458.

[5] C. Zhang., L. Xu and H. Shao. Chaos optimization algorithm based on linear search and its application to nonlinear constraint optimization problems. *Chinese Journal of Control and Decision* **16** (1) (2001) 123–128.

[6] R. Bououden and M-S. Abdelouahab. Chaotic Optimization Algorithm Based on the Modified Probability Density Function of Lozi Map. *Boletim da Sociedade Paranaense de Matemática* doi:10.5269/bspm.41668.

[7] V. T. Jovanovic. Chaotic descent method and fractal conjecture. *Internat. J. Numer. Methods Eng* **48** (1) (2000) 137–152.

[8] Z. Povalej. Quasi-Newton's method for multi objective optimization. *J. Comput. Appl. Math* **255** (2014) 765–777.

[9] J. Liu and S.J. Li. New hybrid conjugate gradient method for unconstrained optimization. *Appl. Math. Comput* **245** (2014) 36–43.

[10] T.W.C. Chen and V. S. Vassiliadis . Solution of general nonlinear optimization problems using the penalty/ modified barrier method with the use of exact hessians. *Comput. Chem. Eng* **27** (4) (2003) 501–525.

[11] E. Canale., F. Robledo., P. Romero and P. Sartor. Monte Carlo methods in diameter-constrained reliability. *Opt. Switch. Netw* **14** (2) (2014) 134–148.

[12] J. A.T. Machado. Optimal tuning of fractional controllers using genetic algorithms. *Nonlinear Dyn* **62** (12) (2010) 447–452.

[13] D. Bunnag and M. Sun. Genetic algorithm for constrained global optimization in continuous variables. *Appl. Math. Comput* **171** (1) (2005) 604–636.

[14] B. Li and W. S. Jiang. Chaos optimization method and its application. *Journal of Control Theory and Application* **14** (4) (1997) 613–615.

[15] C. Choi and J. J. Lee. Chaotic local search algorithm. *Artificial Life and Robotics* **2** (1) (1998) 41–47.

[16] C. Jiang., L. Xu and H. Shao. Chaos optimization algorithm based on linear search and its application to nonlinear constraint optimization problems. *Chinese Journal of Control and Decision* **16** (1) (2001) 123–128.

[17] D.Yang., Z.Liu and J. Zhou. Chaos optimization algorithms based on chaotic maps with different probability distribution and search speed for global optimization. *Commun Nonlinear Sci Numer Simulat* **19** (1) (2014) 1229-1246.

[18] M. Hénon. A two dimensional mapping with a strange attractor. *Commun Math Phys* **50** (1) (1976) 69–77.

[19] R. Lozi. Un attracteur étrange du type attracteur de Hénon. *Journal de Physique. Colloque C5, Supplément* **8** (39) (1978) 9–10.